Learning Feature Representation of Iberian Ceramics with Automatic Classification Models

Pablo Navarro[a,b,*], Celia Cintas[c], Manuel Lucena[d,*], José Manuel Fuertes[d], Claudio Delrieux[e], Manuel Molinos[f]

[a] *Instituto Patagónico de Ciencias Sociales y Humanas. Centro Nacional Patagónico, CONICET, Puerto Madryn, Argentina.*
[b] *Departamento de Informática (DIT), Facultad de Ingeniería, Universidad Nacional de la Patagonia San Juan Bosco. Trelew Chubut, Argentina.*
[c] *IBM Research Africa, Nairobi, Kenya.*
[d] *Department of Computer Science, University of Jaén, Spain.*
[e] *Departamento de Ingeniería Eléctrica y de Computadoras, Universidad Nacional del Sur, and CONICET, Bahía Blanca, Argentina.*
[f] *Research University Institute for Iberian Archaeology, University of Jaén, Spain.*

Abstract

In Cultural Heritage inquiries, a common requirement is to establish time-based trends between archaeological artifacts belonging to different periods of a given culture, enabling among other things to determine chronological inferences with higher precision. Among these artifacts, pottery vessels are significantly useful, given their relative abundance in most archaeological sites. However, this very abundance makes difficult and complex an accurate representation, since no two of these artifacts are identical, and therefore classification criteria must be justified and applied. For this purpose, in this work we propose the use of deep learning architectures to extract automatically learned

features without prior knowledge or engineered features. By means of transfer learning, a Residual Neural Network was retrained with a binary image database of Iberian wheel-made pottery vessels' profiles. These vessels pertain to archaeological sites located in the upper valley of the Guadalquivir River (Spain). The resulting model is able to provide an accurate feature representation space, which is able to classify profile images automatically, achieving a mean accuracy of 0.98. This accuracy is remarkably higher as compared with other state of the art machine learning approaches, where several feature extraction techniques were applied together with multiple classifier models. Furthermore, we show the relevance of introspection in our automatic feature extraction method prior to classification, and the effects of poor feature selection. These results provide novel approaches to current research in automatic feature representation and classification of different objects of study within the Archaeology domain.

Keywords:
Representation Learning, Iberian Pottery, Deep Learning

1. Introduction

One of the most common activities for archaeologists is the study of ceramic artifacts. In general, these objects are short-lived material present in the vast majority of the archaeological sites. On analyzing their properties, researchers can infer their purpose, and establish chronological aspects as well as manufacturing techniques. Therefore, ceramic objects can be very useful to study ethnic groups, their economic organization and relationships, trading routes, and cultural interactions. Ceramic vessels are a particularly interesting case, because their shape and decoration present large variations along time, giving researchers a basis for establishing chronologies among archaeological strata, and providing insights related with trading route analysis, local production, consumer behavior and trends, etc. (**??**). In this context, the ability to analyze and compare ceramic artifacts quantitatively has become a very significant topic in modern Archaeology, given the affordability of digital scanning, and the availability of computing systems with high processing and storing capabilities.

Researchers have proposed several typologies, regarding different criteria to facilitate the study of the material (**?**). Since each typology pays attention to vessel features in a different way, these classifications hardly contribute to the homogenization of pottery shape analysis. This raises the need for archaeologists to have standardized and objective shape metrics, which can also serve in automatic analysis and classification of large vessel collections. Trying to address this problem, recently several automated processing tools for large archaeological datasets have been proposed (**????**).

In particular, vessel profiles have been used for characterization of wheel-made pottery for a long time (**??**), but the first attempts to manage them with computer systems are more recent. **?**, propose a parametric representation method, mostly aimed to visualization and archiving. Also, profile comparison methods have been suggested, using specific distance metrics among given profiles. For instance, (**?**) proposes to compute a distance metric based on overlap maximization among profiles. This metric is however

*Corresponding authors: Tel.: +549-280-457-4254
emails: pnavarro@cenpat-conicet.gob.ar (Pablo Navarro), mlucena@ujaen.es (Manuel Lucena)

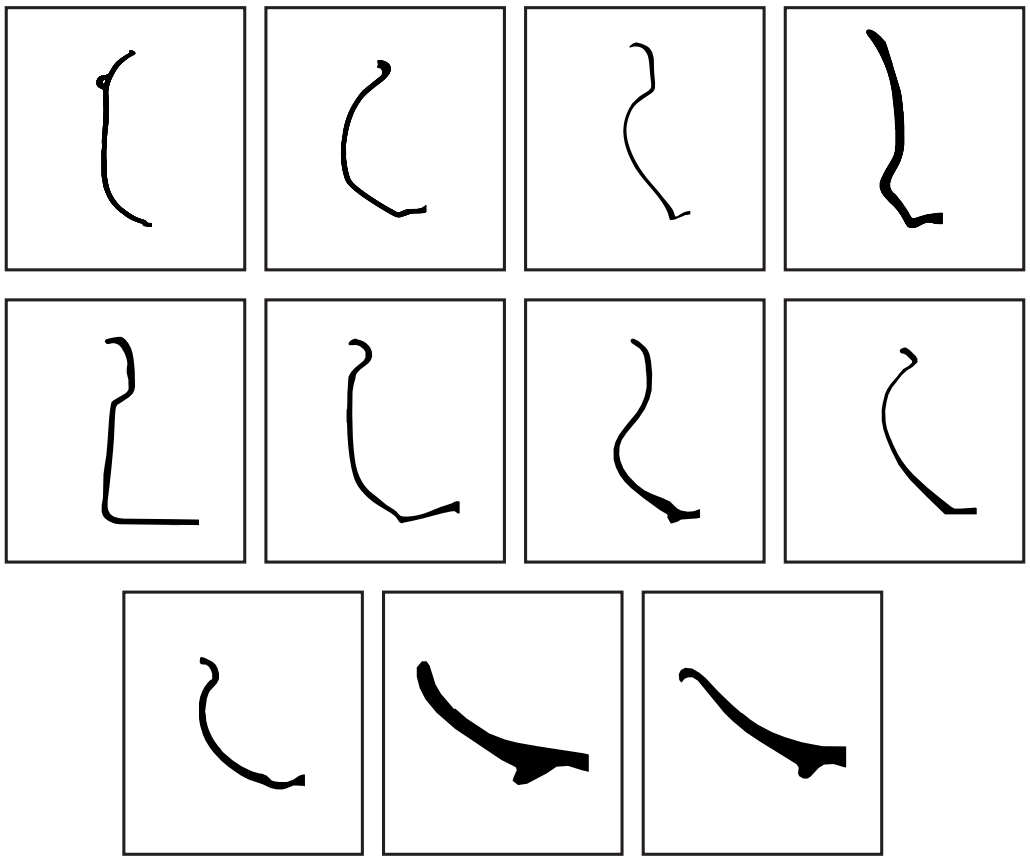

Figure 1: Binary profile samples of Iberian wheel-made pottery collected at several archaeological sites located in the upper valley of the Guadalquivir River (Spain). An experts group established specific morphological criteria that lead to these 11 reference classes, of which nine correspond to closed shapes and the other two to open ones (**?**). More detail regarding the characteristics of the dataset can be found in Section 3.1.

more adequate for solid objects, but fails for vessels (**?**). Subsequent proposals based on other known local features(**?**), shape context descriptors (**?**), are also combined with multivariate analyses to establish comparisons among vessels' shapes. Other approaches (**???**) rely on a continuous profile shape interpolation, characterizing profiles by means of their radii, tangents and curvatures along the contour.

On the other hand, Deep Learning (DL) methods are becoming widespread in many research areas, enabled by the capability of current commodity hardware acceleration and flexible libraries for an effective design and test of models. Archaeology is not an exception, and DL methods applied to problems in this field such as object identification and feature extraction is becoming a common practice. **?** propose a method for recognizing modeling style in Bodhisattva's head images based on a very deep convolutional network developed for large-scale image recognition (VGGNet), with a two-step recognition method for their modeling style: feature extraction utilizing VGGNet and clustering

with K-means algorithm. In **?** a unsupervised feature learning with K-means, inspired by deep learning, was employed to extract art features without any prior information about their nature or the stylistic designation for classify style paintings. Furthermore, **?** present automatic techniques for sorting tasks of digital documentation of architectural heritage. **?** present a convolutional neural network for automatic feature extraction and classification of wheel-made Iberian pottery profiles, but no introspection regarding the representation space and its quality is assessed, limiting the usefulness of the method notwithstanding its high accuracy.

2. Research aim

This paper presents a novel automatic identification system for Iberian ceramic materials based on the complete fragments collected in various deposits by applying machine learning techniques. From a digitized profile, the system can determine the category to which the ceramic vessel is from with high precision. This system mainly provides relevant data on the category of ceramics to experts in both the excavation and laboratory phases, which helps them determine connections between found deposits, commercial routes, processing techniques, and provide relevant cues in other archeological research questions.

Also, a novel feature of our approach is that it generates a feature space in which metric distance is closely related to vessel shape similitude. In other words, this representation allows to identify which shapes of a given vessel is nearer or farther. This property is being quite informative to the archaeologists, and is helping them create new vessel classification categories based on grouping in this feature space. Furthermore, the use of transfer learning creates new, flexible representations, which are more realistic and with more discriminative power, and can be extended to other historical periods other than Iberic. A generalized application of these deep learning techniques in Archaeology will new and fruitful research lines of high interest and scientific value.

3. Materials and Methods

We propose the use of an automatically generated feature space arising in the last convolutional layer from a pre-trained network through transfer learning from `ResNet-18` (**?**). This feature space is proven to be able to group the most important features of pottery vessels. Furthermore, we will compare the space generated with other methods to evaluate the effectiveness of the spaces in vessel classification. In this section we present the pipeline required to generate and compare the feature spaces for three different feature types. The first one is based on Principal Component Analysis (PCA) on raw pixels, with four component sizes (600, 800, 900 and 1000), the second one uses the custom CNN network trained in (**?**) and the last approach is based on transfer learning with `ResNet-18` and retraining for pottery classification. Also, raw-pixel based classification was tested as a baseline to assess the effects of feature selection in classification.

The general processing pipeline of our experiments consists of four stages. First, we preprocess the vessel profile images by normalizing and downsampling them to a fixed pixel dimension 224×224 prior to use PCA, `ResNet-18` and raw pixel classification methods. For the custom CNN, the images are downsampled to 64×64, as this is a

requirement for this architecture. Second, we apply a feature extraction process to the mentioned images to establish a baseline for comparison with traditional feature-based image classification. Third, we extract the last convolutional layer from the custom network and our approach based on `ResNet-18`. This process produces one feature space per approach. Fig. 2 shows a UMAP visualization with the features spaces of `ResNet-18` and Custom CNN, and Fig. 3 depicts a visualization for raw-pixel-based and PCA with 1000 components. Finally, the fourth step is to employ the extracted features to train different classifiers, in particular, Support Vector Machines (SVM) (**?**) and Random Forest Classifier (RFC) (**??**).

3.1. Dataset

To perform the experiments we use as input data the pixel information from binary profile images database. The profiles images correspond to domain experts' drawings from Iberian wheel-made vessels collected in various archaeological sites located along the upper valley of the Guadalquivir River (Spain). The vessels can be classified into eleven different classes based on the shape. These include the forms of the lip, neck, body, base, and handles, and the relative ratios between their sizes. Nine of these classes corresepond to closed vessel shapes, while the two other belong to open ones (**?**) (see Fig. 1 for a graphical representation of the mentioned shapes).

The profile database consists of images of a profile view of the vessels with different pixels resolution and size scale. These variabilities are associated with the acquisition process of each sample. Images that were not previously classified by experts were not considered. The final dataset included 1282 labeled images, and was split into three subsets corresponding to training (with 898 images, represent the 70% of the total dataset), validation (128 images, 10%), and test set (256, 20%). This split was generated using a random-based permutation iterator.

3.2. Feature Extraction

We are interested in exploring which are the best methods for feature representation regarding pottery classification and the impact on the classification performance when the feature extraction process changes. In this subsection we explore one baseline method (raw pixels space), two benchmark approaches: linear feature extraction with PCA (**?**) and last Convolution Layer from custom network (**?**), as compared with a new proposed approach based on transfer learning techniques from `ResNet-18`. Also, we describe the process of retraining the residual neural network with the profiles pottery samples.

Raw Pixels. The basic representation of the profile pottery vessels is using the raw pixels obtained from the images. Each sample is formed by a single-channel image of size 224×224 pixels. Images were resized to fit this size by means of bilinear downsampling during preprocessing step, and brightness values were linearly scaled to a $[0, 1]$ range (see Fig. 1). Each matrix is reshaped to a 1D vector to be feed into the different classification models.

Linear Feature Extraction. Linear feature extraction methods like Principal Component Analysis or Singular Value Decomposition define an orthogonal transformation to convert the input data into a set of values of uncorrelated variables (the principal components).

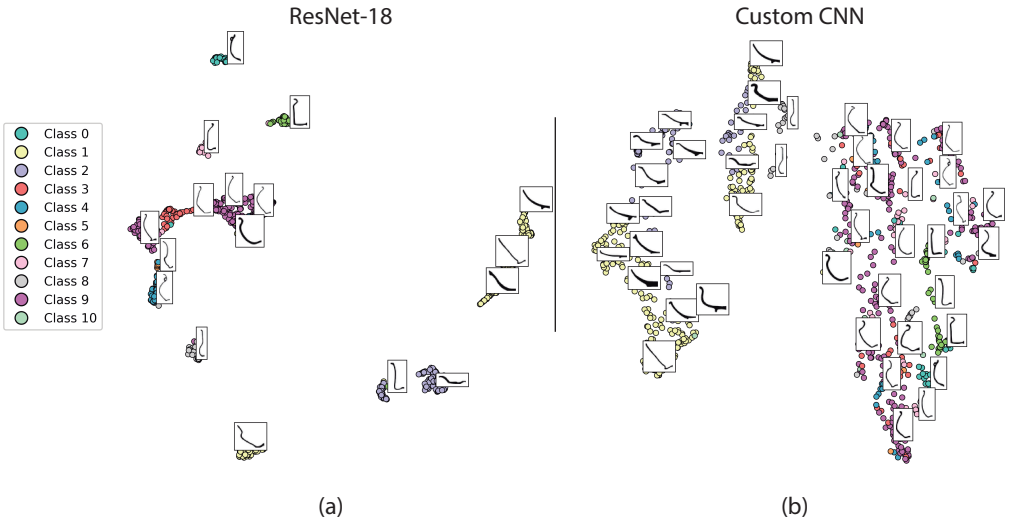

Figure 2: UMAP visualization for the different feature representation spaces generated by neural networks: (a) retrained ResNet-18 for vessel classification, (b) the proposal by **?**. In the feature space generated by the retrained ResNet-18 the vessels present a much better grouping than in the space generated by the Custom CNN approach.

These new variables are linear combinations of the original variables in which the data were expressed. The transformation is defined in such a way that the first principal component explains the largest possible amount of variance in the original dataset. Each principal component can be regarded as a linearly independent feature. Dimension reduction can be performed by retaining the amount of principal components that explains the desired variance. In our case we extracted 600, 800, 900 and 1000 features, with a respective explained variance of 0.985, 0.994, 0.997, 0.999.

Last Convolutional Layer Representation. A noteworthy aspect of neural networks is that the complexity of the patterns that the network represents increases from the initial layers to the output ones. In convolutional networks, this complexity typically arises in relevant geometrical patterns that the network was able to discover after the training process. A useful practice is then to take advantage of this implicit feature extraction, withdrawing the final densely connected layers in a regular CNN and using the last convolutional layer activation as a feature space. In our case we used a custom CNN previously trained for pottery classification (see **?** for details on the architecture, data augmentation techniques and training setup). The resulting feature vector consist of $128x16x16$ trained nodes.

Transfer Knowledge from ResNet-18 network. This approach uses transfer learning (**?**) to extract pretrained weights from other networks with different purposes. This technique allows the use of knowledge acquired with larger networks trained with massive datasets, to resolve a singular problem with small data and limited hardware. This is important in the archaeology space, where the sample set is in most cases limited by

Table 1: Precision, f_1 and recall over the test set for SVM and RFC with each variant of feature representation methods. For the custom CNN trained from scratch we used the implementation presented at (**?**). Our approach uses transfer learning from ResNet-18 (**?**) and retrain for the pottery classification purposes. More details on how the models were trained at Section 3.2.

Method		SVM			RFC		
		Precision	f_1	Recall	Precision	f_1	Recall
ResNet-18		**0.98 (± 0.02)**	**0.96 (± 0.02)**	**0.95 (± 0.03)**	**0.87 (± 0.04)**	**0.81 (± 0.06)**	**0.81 (± 0.04)**
Custom CNN		0.82 (± 0.07)	0.72 (± 0.05)	0.71 (± 0.04)	0.51 (± 0.09)	0.35 (± 0.03)	0.35 (± 0.03)
Raw Pixels		0.69 (± 0.08)	0.60 (± 0.05)	0.59 (± 0.05)	0.44 (± 0.04)	0.39 (± 0.03)	0.41 (± 0.04)
PCA	600	0.59 (± 0.08)	0.35 (± 0.06)	0.33 (± 0.05)	0.23 (± 0.09)	0.15 (± 0.04)	0.19 (± 0.01)
	800	0.62 (± 0.09)	0.37 (± 0.06)	0.35 (± 0.04)	0.21 (± 0.08)	0.15 (± 0.03)	0.19 (± 0.02)
	900	0.66 (± 0.12)	0.40 (± 0.07)	0.36 (± 0.05)	0.19 (± 0.01)	0.15 (± 0.03)	0.19 (± 0.01)
	1000	0.75 (± 0.01)	0.47 (± 0.07)	0.42 (± 0.06)	0.20 (± 0.01)	0.15 (± 0.02)	0.19 (± 0.02)
Mathematical Morphology		0.62 (± 0.4)	0.52 (± 0.04)	0.52 (± 0.04)	0.59 (± 0.10)	0.55 (± 0.03)	0.55(± 0.01)

the number of discoveries. Furthermore, this type of process allows training networks in fewer steps, reducing time and computation costs.

In this work, we used the `ResNet-18` architecture (**?**) pretrained with the ImageNet dataset (**?**) for object classification in 1000 classes (for example dogs, people, houses, cats, etc.) with 3.2 million images in total. We modified the last fully connected layer adding a linear layer (512 to 11) and a logarithmic softmax layer (see Fig. 4). After this, the resulting network was retrained for 100 epochs with the vessel dataset (see Subsection 3.1) using cross-entropy as loss function, a learning rate $2x10^{-3}$ with a batch size of 32. We applied data augmentation, particularly two types of affine transformations with a probability of 0.7 of being scaled (between 0.7 and 1.0) and with the same probability of being flipped horizontally. We used ADAM optimization (**?**) with $\beta_1 = 0.5$ and $\beta_2 = 0.999$. After training, the feature vector is extracted from the last block of layers of the ResNet-18 (output size: $512x4x4$) trained with vessel profiles. A UMAP visualization (**?**) of this feature space can be seen in Fig. 2(a).

3.3. Classification

For the classification stage, different models were trained using the feature extraction techniques shown in the previous Subsection. As a baseline we trained a SVM and RFC, which are the state-of-the-art classifiers proven to perform accurately in many applications(**????**).

Support Vector Machines (SVM). SVMs are based on obtaining an optimal separation hyperplane among a set of patterns. For this, the hyperplane is found with the largest margin (*i.e.,* distance to the closest points at each side) (**?**). SVMs can be used also when the patterns are not linearly separable. In this case, the patterns are mapped into a different feature space in which they turn to be separable, using a specific *kernel function*. We trained the SVM model using a kernel radial basis function (RBF) with a coefficient in 0.09.

Random Forest Classifier (RFC). Random Forest Classifier (**?**) can be described as a

Table 2: Precision, f_1, and recall over the test set for different classifier methods. Comparing performances for our approach (with SVM and RFC classifier), the retrain Resnet-18 using all the architecture proposed in (**?**) and the custom CNN using all the architecture (**?**) and SVM/RFC approaches. More details on how the models were trained in Section 3.2. Simplified Curve Method (**?**) and Mathematical Morphology (**?**) were comparing as the classical method.

Method	Precision	f_1	Recall
ResNet-18 (with SVM)	**0.98**	**0.96**	**0.95**
ResNet-18 (with RFC)	0.87	0.81	0.81
ResNet-18 (fine-tune)	0.96	0.95	**0.95**
Custom CNN (with SVM)	0.82	0.72	0.71
Custom CNN (with RFC)	0.51	0.35	0.35
Custom CNN (**?**)	0.91	0.90	0.90
Simplified Curve Method (**?**)	0.79	0.77	0.76
Mathematical Morphology (**?**)	0.80	0.79	0.77

large number of individual decision trees that operate as an ensemble, where each individual tree in the random forest spits out a class prediction, being the model's prediction the most voted class. It uses bagging and feature randomness when building each individual tree and tries to create an uncorrelated forest of trees, whose combined prediction is more accurate than that of any individual tree. We configured the RFC with 500 trees in the forest, each tree with 4 maximum depth to avoid overfitting.

3.4. Evaluation metrics

In this section, we show the process of evaluating the performance of the features and the capacity of the space to represent the vessels. Comparing the UMAP visualization(Figs. 2 and 3), we can see which spaces are more adequate for grouping the vessel class. For one quantitative evaluation, we evaluated the classifiers (SVC and RFC) with three metrics. We evaluated with precision, recall and f_1 using the usual definitions for multiclass classifiers:

$$precision_i = \frac{TP_i}{TP_i + FP_i}, \quad pr = \frac{\sum_i precision_i}{N},$$

$$recall_i = \frac{TP_i}{TP_i + FN_i}, \quad rc = \frac{\sum_i recall_i}{N},$$

$$f_1 = 2 * \frac{pr * rc}{pr + rc},$$

where TP_i, FP_i, FN_i are respectively the amount of true positives, false positives, and false negatives of class i, and N is the amount of classes.

4. Results

For the feature extraction step, UMAP visualization of each different representation approach can be seen in Figs. 2 and 3. In Fig. A1 the representation space of `ResNet-18` without retraining with pottery images is depicted. Is worth noting that with only a small amount of epochs during retraining we largely improve the discriminative feature space for pottery classification. We can assess qualitative the class separation capability of each method to differentiate close and open shape vessels. To validate the obtained representations and the automatic classification methods we assessed the models' quality according to the standard metrics (precision, recall, and f_1) when the model was applied to previously unseen images(see Table 1). These metrics were evaluated by means of the *scikit-learn* library (**?**). We performed five random cross-validation processes, obtaining an average accuracy of 0.98 (sd 0.02) for the best performing feature representation method and classifier combination (in this case, our proposed method and SVM). See Table 1 to assess all the preprocessing techniques combined with SVM and RFC as classification methods.

In Fig. A5 we present the confusion matrix obtained with the *test* dataset ($n = 256$) for all preprocessing methods with SVM as the classifier. In the Supplementary Section, the confusion matrix for RFC is depicted in Fig. A3. Both visualizations were normalized to avoid misleading perceptions due to the unbalance in the pottery classes. It can be noted that our approach for feature representation improves in all classes, as compared with the state of the art CNN, linear dimension reduction techniques and as a baseline no preprocessing step applied.

As an effort to make these methods widespread, our implementation uses open-source platforms including the Python programming language and the PyTorch library (**?**). This allows to take advantage of GPU acceleration during the training stage. The complete code of the project, including the network architecture, transfer learning procedure, retraining, feature extraction and validation of our method is available at[1].

We also evaluated the execution time for the complete pipeline, from preprocessing and feature extraction to training and classification steps. The experiments were performed with an Intel i7-6700K processor and Nvidia 1080 for GPGPU processing. The proposed transfer knowledge method takes 3.73 seconds (± 244 ms) in taking the image and obtain the space feature while the custom CNN takes 3.19 seconds (± 49.3 ms). The training times for the feature representation based on ResNet takes 149 ms (± 22.4 us) with SVM as a classifier, and 1.9 seconds (± 11.7 ms) with RFC, while in the Custom CNN feature takes 639 ms (± 267 us) and 1.84 seconds (± 17.7 ms) respectively. For prediction, the feature based on ResNet needs 44.1 ms for SVM and 32.4 ms for RFC. A more complete description of the required training and classification times of all methods can be seen in Table 3.

5. Discussion and Conclusions

We propose a residual neural network for extracting automatically learned features to enhance current classifiers of Iberian ceramic pottery. Our feature representation

[1] `https://github.com/celiacintas/vasijas/tree/unsupervised`

Table 3: Preprocessing, training and prediction average time for SVM and RFC classifiers across different feature extraction techniques.

Method		Preprocessing Time	SVM		RFC	
			Train Time	Predict Time	Train Time	Predict Time
ResNet-18		3.73 s ± 244 ms	149 ms ± 22.4 μs	**44.1 ms** ± 95 μs	1.9 s ± 11.7 ms	32.4 ms ± 74 μs
Custom CNN		**3.19 s** ± 49.3 ms	639 ms ± 267 μs	167 ms ± 1.14 ms	**1.84 s** ± 17.7 ms	36.2 ms ± 35.1 μs
Raw Pixels		5.53 s ± 2.33 ms	31.5 s ± 789 μs	8.1 s ± 310 μs	3.71 s ± 74.2 ms	56.2 ms ± 62.6 μs
PCA	600	17.5 s ± 40 ms	**1.23 ms** ± 89.6 μs	132 ms ± 9.3 μs	2.15 s ± 1.92 μs	28.2 ms ± 34.9 μs
	800	21.7 s ± 55.3 ms	1.62 s ± 43.5 μs	176 ms ± 11.8 μs	2.47 s ± 7.07 ms	**28 ms** ± 59 μs
	900	23.8 s ± 31.6ms	1.82 ms ± 160 μs	199 ms ± 15.3 μs	2.63 s ± 3.73 ms	28.3 ms ± 19.6 μs
	1000	19.8 s ± 15.5 ms	2.02 s ± 547 μs	223 ms ± 82.7 μs	2.71 s ± 1.62 ms	28.6 ms ± 28.7 μs

technique used as a preprocessing step with classic machine learning models such as SVM outperforms previous classification methods (**????**). Furthermore, is interesting to notice that the proposed method uses transfer learning from a `ResNet-18` and retrains over the vessels dataset for automatic feature extraction representation of pottery objects requires less amount of data and outperform traditional machine learning pipelines and state of the art custom CNNs.

Also, we discuss the relevance of introspection with visualizations such as UMAP in automatic feature extraction methods prior to classification, and the effects of poor feature selection. We compared the quality of several preprocessing methods for feature extraction and their impact on the classification outcome.

The complete implementation was deployed using open source libraries, available on the already mentioned public repository. The proposed solution is adequate for other classification tasks over different kinds of archaeological material with reduced sample size due to the transfer learning properties. As an example, current work is been done for outlining specific stone-made shells used as projectiles (spears, darts, arrows, etc). It also may be used for several other studies, including the analysis of fragments of projectile points or their retouching and reactivation process. Similar applications can be found also for bone fragments and many other topics.

Acknowledgments

This work was supported in part by the Ministerio de Ciencia, Innovación y Universidades and in part by the European Union through the Research Project under Grant RTI2018-099638-B-I00, the Center for Advanced Studies in Information and Communication Technologies (CEATIC) and the Research University Institute for Iberian Archeology of the University of Jaén.

References

Akar, Ö., Güngör, O., 2012. Classification of multispectral images using random forest algorithm. Journal of Geodesy and Geoinformation 1 (2), 105–112.

Belongie, S., Malik, J., Puzicha, J., April 2002. Shape matching and object recognition using shape contexts. IEEE Transactions on Pattern Analysis and Machine Intelligence 24 (4), 509–522.

Breiman, L., 2001. Random forests. Machine learning 45 (1), 5–32.

Cintas, C., Lucena, M., Fuertes, J. M., Delrieux, C., Navarro, P., González-José, R., Molinos, M., 2019. Automatic feature extraction and classification of iberian ceramics based on deep convolutional networks. Journal of Cultural Heritage.

Deng, J., Dong, W., Socher, R., Li, L.-J., Li, K., Fei-Fei, L., 2009. ImageNet: A Large-Scale Hierarchical Image Database: CVPR09.

Gultepe, E., Conturo, T. E., Makrehchi, M., 2018. Predicting and grouping digitized paintings by style using unsupervised feature learning. Journal of cultural heritage 31, 13–23.

He, K., Zhang, X., Ren, S., Sun, J., June 2016. Deep residual learning for image recognition: The IEEE Conference on Computer Vision and Pattern Recognition (CVPR).

Joachims, T., 1998. Text categorization with Support Vector Machines: Learning with many relevant features. Springer, Berlin, Heidelberg, pp. 137–142.
URL: http://link.springer.com/10.1007/BFb0026683
DOI: 10.1007/BFb0026683

Kampel, M., Sablatnig, R., 2003. An automated pottery archival and reconstruction system. Journal of Visualization and Computer Animation 14 (3), 111–120.

Karasik, A., Smilansky, U., 2011. Computerized morphological classification of ceramics. Journal of Archaeological Science 38 (10), 2644 – 2657.

Kingma, D. P., Ba, J., 2014. Adam: A method for stochastic optimization. arXiv preprint arXiv:1412.6980.

Llamas, J., Lerones, P. M., Zalama, E., Gómez-García-Bermejo, J., 2016. Applying deep learning techniques to cultural heritage images within the INCEPTION project: Lecture Notes in Computer Science (including subseries Lecture Notes in Artificial Intelligence and Lecture Notes in Bioinformatics). Vol. 10059 LNCS. pp. 25–32.
DOI: 10.1007/978-3-319-48974-2_4

Lucena, M., Fuertes, J. M., Martinez-Carrillo, A. L., Ruiz, A., Carrascosa, F., 2016. Efficient classification of Iberian ceramics using simplified curves. Journal of Cultural Heritage 19, 538–543.
DOI: 10.1016/j.culher.2015.10.007

Lucena, M., Fuertes, J. M., Martínez-Carrillo, A. L., Ruiz, A., Carrascosa, F., Oct 2017. Classification of archaeological pottery profiles using modal analysis. Multimedia Tools and Applications 76 (20), 21565–21577.
URL: https://doi.org/10.1007/s11042-016-4076-9
DOI: 10.1007/s11042-016-4076-9

Lucena, M., Martínez-Carrillo, A. L., Fuertes, J., Carrascosa, F., Ruiz, A., 2014. Decision support system for classifying archaeological pottery profiles based on mathematical morphology. Multimedia Tools and its Applications.
DOI: 10.1007/s11042-014-2063-6

Maaten, L., Lange, G., Boon, P., 2009. Visualization and automatic typology construction of pottery profiles: Frischer, B. (Ed.), Making history interactive: computer applications and quantitative methods in archaeology (CAA). Vol. 2079 of BAR International Series. Archaeopress, Oxford u.a., pp. 356–362.

Makridis, M., Daras, P., Jan. 2013. Automatic classification of archaeological pottery sherds. J. Comput. Cult. Herit. 5 (4), 15:1–15:21.
URL: http://doi.acm.org/10.1145/2399180.2399183
DOI: 10.1145/2399180.2399183

McInnes, L., Healy, J., Melville, J., 2018. Umap: Uniform manifold approximation and projection for dimension reduction. arXiv preprint arXiv:1802.03426.

Menze, B. H., Ur, J. A., Aug 2014. Multitemporal fusion for the detection of static spatial patterns in multispectral satellite images—with application to archaeological survey. IEEE Journal of Selected Topics in Applied Earth Observations and Remote Sensing 7 (8), 3513–3524.
DOI: 10.1109/JSTARS.2014.2332492

Mom, V., 2007a. SECANTO - The SECtion Analysis TOol: Figueiredo, A., Velho, G. L. (Eds.), The world is in your eyes. CAA2005. Computer Applications and Quantitative Methods in Archaeology. Tomar, Portugal, pp. 95–101.

Mom, V., 2007b. Where did i see you before... a holistic method to compare and find archaeological artifacts: Decker, R., Lenz, H. J. (Eds.), Advances in Data Analysis. Springer Berlin Heidelberg, Berlin, Heidelberg, pp. 671–680.

Nautiyal, V., Kaushik, V. D., Pathak, V. K., Dhande, S., Nautiyal, S., Naithani, M., Juyal, S., Gupta, R. K., Vasisth, A. K., Verna, K. K., Singh, A., 2006. Geometric modeling of indian archaeological pottery: A preliminary study: Clark, J., Hagemeister, E. (Eds.), Exploring New Frontiers in Human

Heritage. CAA2006. Computer Applications and Quantitative Methods in Archaeology. Fargo, United States.

Oquab, M., Bottou, L., Laptev, I., Sivic, J., 2014. Learning and transferring mid-level image representations using convolutional neural networks: Proceedings of the IEEE conference on computer vision and pattern recognition. pp. 1717–1724.

Orton, C., Tyers, P., Vinci, A., 1993. Pottery in Archaeology. Cambridge University Press, United Kingdom.

Ozigis, M., Kaduk, J., Jarvis, C., da Conceição Bispo, P., Balzter, H., 2019. Detection of oil pollution impacts on vegetation using multifrequency sar, multispectral images with fuzzy forest and random forest methods. Environmental Pollution, 113360.
URL: http://www.sciencedirect.com/science/article/pii/S0269749119316604
DOI: https://doi.org/10.1016/j.envpol.2019.113360

Paszke, A., Gross, S., Chintala, S., Chanan, G., Yang, E., DeVito, Z., Lin, Z., Desmaison, A., Antiga, L., Lerer, A., 2017. Automatic differentiation in pytorch.

Pedregosa, F., Varoquaux, G., Gramfort, A., Michel, V., Thirion, B., Grisel, O., Blondel, M., Prettenhofer, P., Weiss, R., Dubourg, V., Vanderplas, J., Passos, A., Cournapeau, D., Brucher, M., Perrot, M., Duchesnay, E., 2011. Scikit-learn: Machine learning in Python. Journal of Machine Learning Research 12, 2825–2830.

Pereira Sieso, J., 1989. La cerámica ibérica de la cuenca del Guadalquivir. Trabajos de Prehistoria 46, 149–159.

Piragnolo, M., Masiero, A., Pirotti, F., Apr. 2017. Comparison of Random Forest and Support Vector Machine classifiers using UAV remote sensing imagery: EGU General Assembly Conference Abstracts. Vol. 19 of EGU General Assembly Conference Abstracts. p. 15692.

Rice, P. M., 1987. Pottery Analysis. University of Chicago Press, Chicago.

Saragusti, I., Karasik, A., Sharon, I., Smilansky, U., 2005. Quantitative analysis of shape attributes based on contours and section profiles in artifact analysis. Journal of Archaeological Science 32 (6), 841 – 853.

Shennan, S., Wilcock, J., 1975. Shape and style variation in central german bell beakers. Science and Archaeology 15, 17–31.

Smith, N. G., Karasik, A., Narayanan, T., Olson, E. S., Smilansky, U., Levy, T. E., Mar 2014. The pottery informatics query database: A new method for mathematic and quantitative analyses of large regional ceramic datasets. Journal of Archaeological Method and Theory 21 (1), 212–250.
URL: https://doi.org/10.1007/s10816-012-9148-1
DOI: 10.1007/s10816-012-9148-1

Vapnik, V., 2013. The nature of statistical learning theory. Springer science & business media.

Wang, H., He, Z., Huang, Y., Chen, D., Zhou, Z., 2017. Bodhisattva head images modeling style recognition of Dazu Rock Carvings based on deep convolutional network. Journal of Cultural Heritage 27, 60–71.
DOI: 10.1016/j.culher.2017.03.006

Wold, S., Esbensen, K., Geladi, P., 1987. Principal component analysis. Chemometrics and Intelligent Laboratory Systems 2 (1), 37 – 52, proceedings of the Multivariate Statistical Workshop for Geologists and Geochemists.
URL: http://www.sciencedirect.com/science/article/pii/0169743987800849
DOI: https://doi.org/10.1016/0169-7439(87)80084-9

Appendix

To analize the improvement of transfer learning and retraining to specific tasks we visualize `ResNet-18` without retraining in Fig. A1.

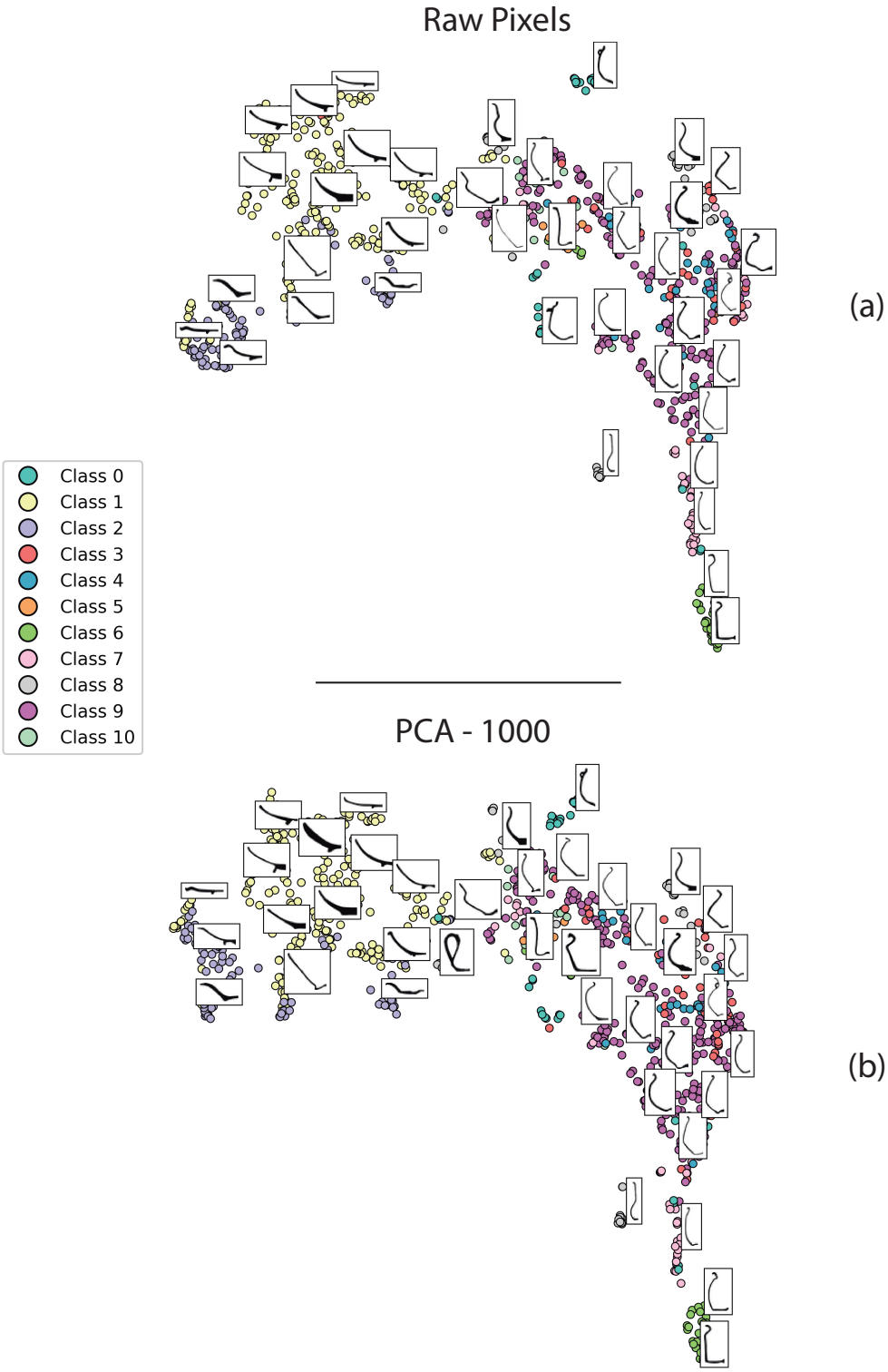

Figure 3: UMAP visualization for feature representation space comparison between raw pixel values and linear feature extraction method been applied to the dataset : (a) Raw pixel feature-based classification. (b) PCA with 1000 PCs (See Fig. A4 for 600, 800 and 900 PCs). The distribution of the samples in both feature spaces is very similar, with poorly defined clusters. Nevertheless, we can see that in both cases *open vessels* (left) and *closed vessels* (right) are separated.

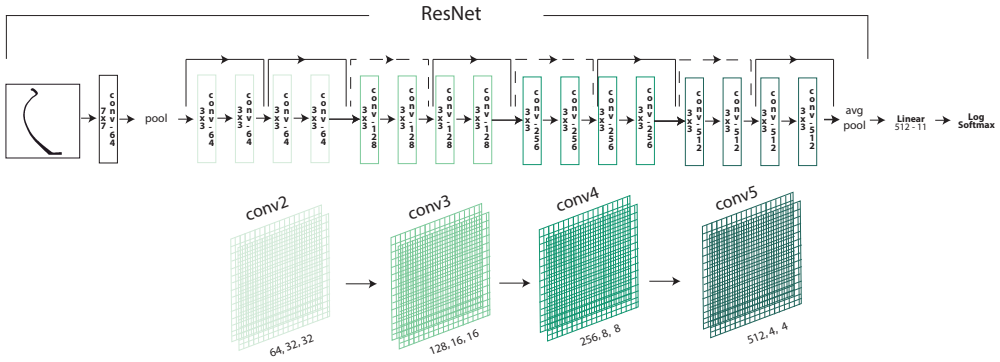

Figure 4: Network Architecture based on ResNet-18 (**?**) for retraining under the specific task of pottery classification. The arrows between non consecutive layers represent residual connections, and the dashed ones represent dimensionality increments.

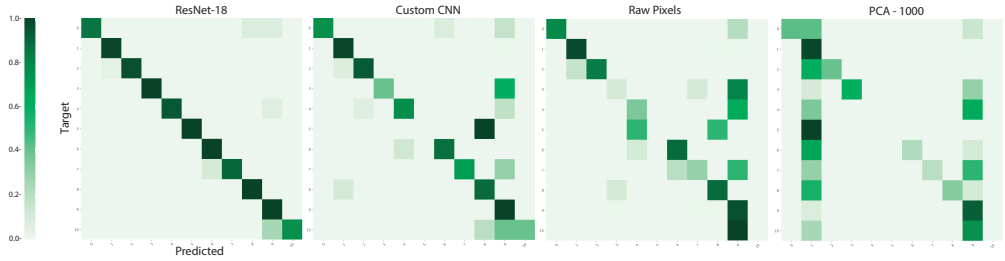

Figure 5: Normalized confusion matrix of the predicted results of the SVM across different feature representation approaches over a randomized test dataset of vessels images ($n = 256$). Best results are clearly achieved by the retrained ResNet-18 across the 11 vessels classes, while poorest results come from PCA-1000 feature space.

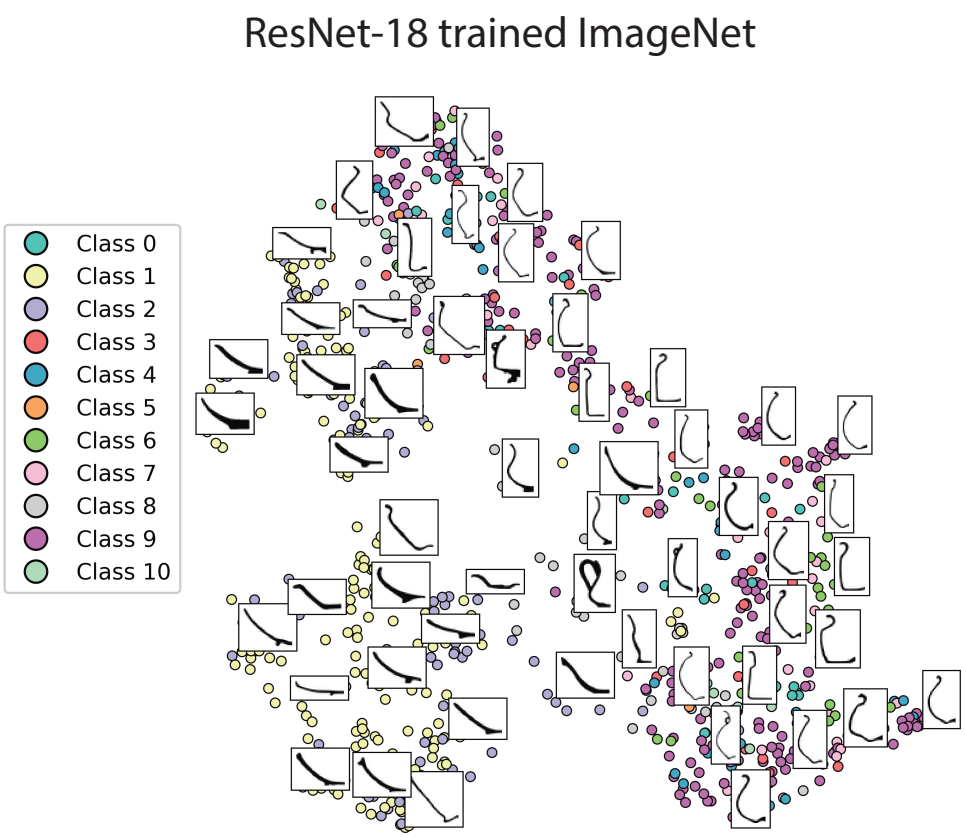

Figure A1: UMAP visualization for ResNet-18 pretrained model with Image Net Dataset. We can compare the feature space with and without retraining for our specific dataset and pottery classification task in Fig. 2. With only a few more iterations of the network we can see a large improvement in the dicriminative properties of the generated feature space.

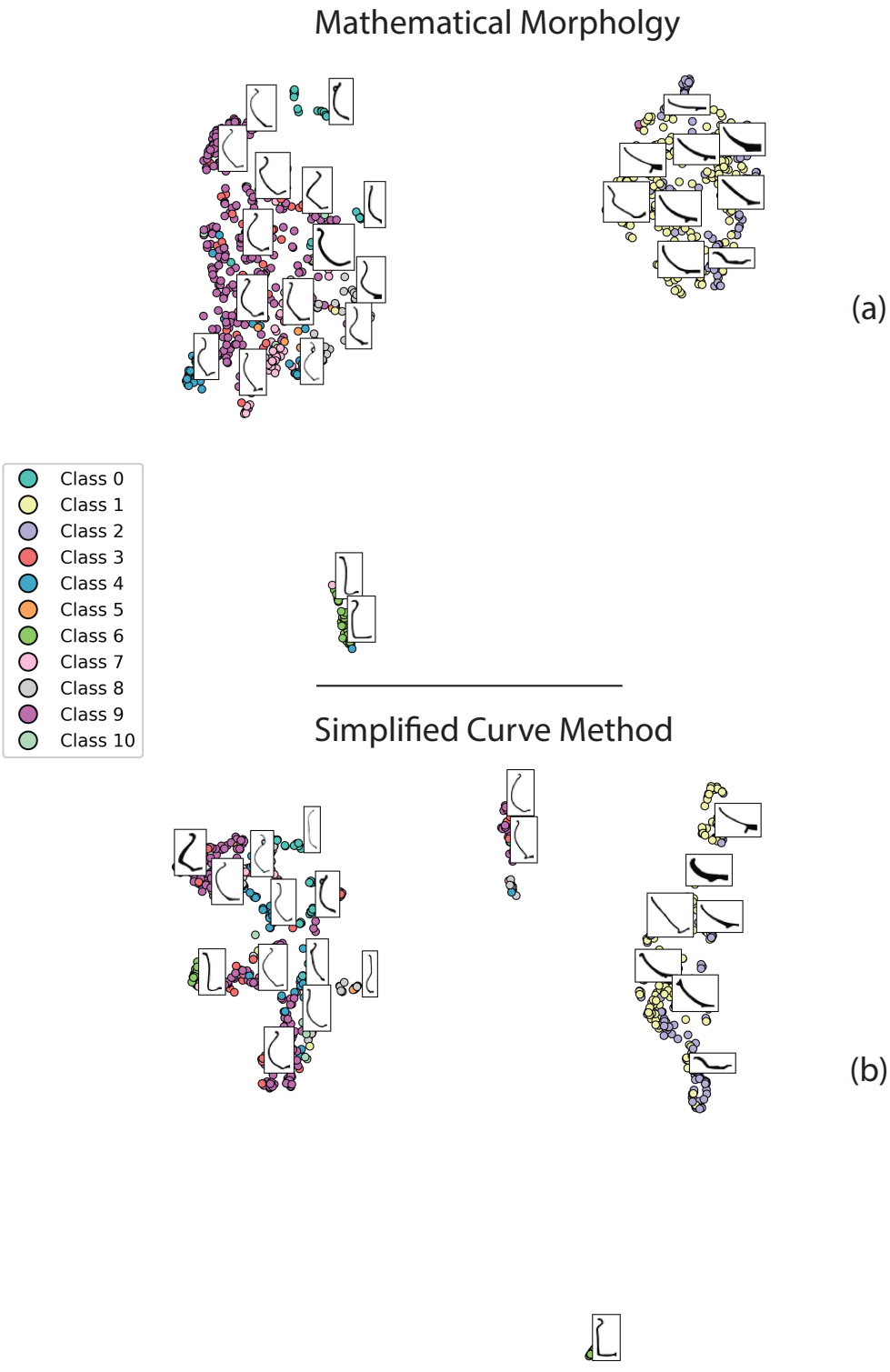

Figure A2: UMAP visualization for.

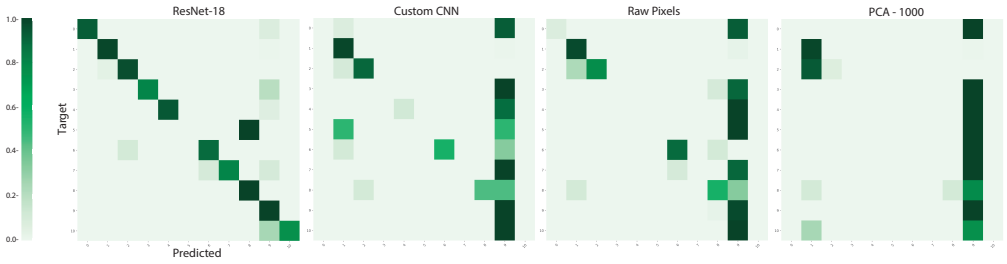

Figure A3: Normalized confusion Matrix of the predicted results of the RFC across different feature representation approaches over a randomized test dataset of vessels images ($n = 256$).

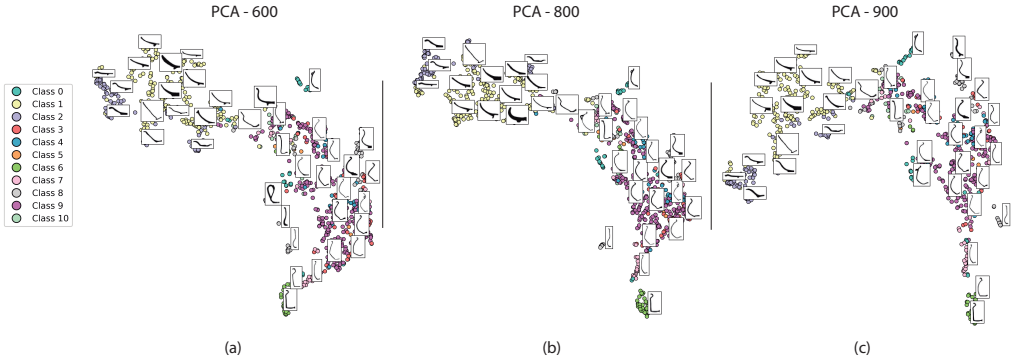

Figure A4: UMAP visualization for PCA features.

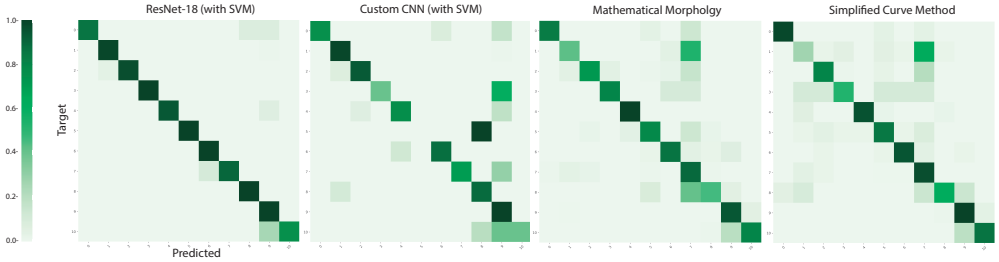

Figure A5: Normalized confusion matrix of the predicted results of the classification approaches over a the same dataset of vessels images, For more detail of the performance for the methods see Table 2.

.